AN ASSUMED STRESS HYBRID FINITE ELEMENT MODEL FOR THE ANALYSIS OF AN AXISYMMETRIC THICK WALLED PRESSURE VESSEL

T.V.S.R. APPA RAO,

Structural Engineering Research Regional Centre, Madras, India

ABSTRACT

An assumed stress hybrid finite element model for the analysis of axisymmetric solids has been presented and stiffness matrices for triangular and quadrilateral elements are formulated using the principle of minimum complementary energy. A thick sphere and an infinitely long thick cylinder subjected to internal pressure are analyzed by using the assumed stress hybrid model. The stress pattern obtained by using the assumed stress hybrid model is compared with the exact solution and with the stress pattern obtained by using the well known displacement assumption model. The comparison shows that the stress pattern obtained by using the assumed stress hybrid model is somewhat better than the one obtained by using the displacement assumption model.

1. INTRODUCTION

Clough and Rashid [1] have developed an assumed displacement triangular ring finite element model for the analysis of axisymmetric solids and they have used the principle of minimum potential energy for the derivation of the element stiffness matrix. This model was used, primarily, for the analysis of solid propellent grains, and was later employed for the analysis of rocket nozzles, spacecraft heat shields, prestressed concrete reactor vessels, and reactor containment structures. The triangular ring element has been found to be a very useful model for the analysis of arbitrary shaped axisymmetric solids. Wilson [2] has extended the formulation to take into account nonaxisymmetric loading.

Applications of the above mentioned finite element model to various problems have shown in their results for stresses at the centroids of the elements a certain amount of oscillation around their true values. To avoid this difficulty, various forms of averaging of stresses have been used. Clough [3] uses a weighted averaging procedure for obtaining stresses at nodes and Zienkiewicz [4] & [5] uses the average of stresses of two adjacent triangular elements.

Pian [6] has shown a different method of deriving element stiffness matrices based on the principle of minimum complementary energy. In this method, stresses are assumed in the element and the boundary compatability is achieved by prescribing a simple displacement pattern along the inter-element boundaries. Element stiffness matrices based on the above mentioned formulation - "Assumed Stress Hybrid Model" - have been applied to plane stress [6], [7] and plate bending problems [8], [9] . Pian [9] has concluded that the use of the assumed stress hybrid model will yield a structure which is more flexible than the compatable model of the same boundary displacement approximation and more rigid than the equilibrium model of the same internal stress approximation. Further, he has stated that the finite element method based on the assumed stresses can provide more accurate stress estimation than the assumed displacement schemes.

In this report, an assumed stress hybrid model for the triangle and arbitrary quadrilateral ring element stiffness matrices has been formulated for the analysis of arbitrary shaped axisymmetric solids. Most of the functions assumed for the stress pattern in the elements are the same as those which occur in the classical theory of thick cylinder and thick sphere. A thick sphere and an infinitely long thick cylinder subjected to internal pressure have been analyzed by using the stress hybrid model. Results of the investigation have been compared with those computed by using the displacement model of an axisymmetric triangular ring element and with the exact solution. Relative merits of the assumed stress hybrid model and the displacement assumption model are discussed in this report.

2. GENERAL

To analyze a structure using the finite element method the structure is idealized into a set of discrete elements connected only at finite number of points known as the nodal points. The discrete elements may be one dimensional or two dimensional or three dimensional depending on the type of the structure. Either displacements or forces at nodes are suitably chosen as the unknowns in the analysis. When the displacements at the nodes are the unknowns in the problem, a stiffness matrix for the element, which relates the nodal forces to the nodal displacements, is derived from the assumption of either a displacement field or a stress field in the element. Using the element stiffness matrices a set of simultaneous linear algebric equations with nodal displacements as the unknowns can be obtained when the equilibrium of forces at each node is established. After solving the equations for the unknown displacements, stresses and displacements over the entire structure can be easily determined.

In this report, stiffness matrices for the triangular and arbitrary quadrilateral ring elements (Figs. 1a and 2a) are formulated from the assumption of a stress pattern in the elements. Idealizations of an axisymmetric structure (i) into a set of triangular ring elements, and (ii) into a set of arbitrary quadrilateral elements are shown in Figs. 1 and 2 respectively.

3. ASSUMED STRESS HYBRID MODEL

Stiffness matrix of an element can be determined by expressing the strain energy U in terms of the nodal displacements $\{q\}$ and the element stiffness matrix $[k]$ as:

$$U = \frac{1}{2} \lfloor q \rfloor [k] \{q\} \tag{1}$$

The internal strain energy U can also be expressed in terms of the stresses $\{\sigma\}$ as:

$$U = \frac{1}{2} \int_V \lfloor \sigma \rfloor [N] \{\sigma\} dv \tag{2}$$

where the matrix $[N]$ relates the strains $\{\epsilon\}$ and stresses $\{\sigma\}$ as in the following equation:

$$\{\epsilon\} = [N] \{\sigma\} \tag{3}$$

Now, to determine the stress distribution in the element a set of nodal displacements is chosen and a simple displacement pattern is prescribed on the boundary, A_2. The problem of determining the stress distribution can be solved by using the principle of minimum complementary energy [10] which may be stated as:

$$\pi_c = U - \int_{A_2} u_i S_i \, dA \qquad = \text{minimum} \tag{4}$$

where U is the strain energy expressed in terms of stress components σ_{ij}, u_i are the components of the prescribed displacements, and S_i are the components of surface forces which are related to the stress components by:

$$S_i = \sigma_{ij} \ n_j \tag{5}$$

where n_j are the direction cosines of the surface normal. To apply the variational principle, stresses $\{\sigma\}$ are expressed in terms of m undetermined coefficients $\{\beta\}$ as:

$$\{\sigma\} = [P] \{\beta\} \tag{6}$$

where the terms of the matrix $[P]$ are functions of the coordinates. The number of elements in $\{\beta\}$ is unlimited.

By expressing $\{\sigma\}$ in terms of $\{\beta\}$ in eq.(2), the internal strain energy can be written as:

$$U = \frac{1}{2} \lfloor\beta\rfloor [H] \{\beta\} \tag{7}$$

where
$$[H] = \int_V [P^T] [N] [P] dv \tag{8}$$

it can be seen that $[H]$ is symmetrical.

The prescribed displacements on the boundary A_2 are given in terms of the generalized displacements $\{q\}$ at nodes as:

$$\{u\} = [L] \{q\} \tag{9}$$

where the terms in the matrix $[L]$ contain coordinates on the surface.

Using eqs.(5) and (6), surface forces $\{S\}$ can be related to the undetermined stress coefficients $\{\beta\}$ as:

$$\{S\} = [R] \{\beta\} \tag{10}$$

where the terms in $[R]$ contain the coordinates on the surface.

Then, the total complementary energy is given by:

$$\pi_c = \frac{1}{2} \lfloor\beta\rfloor [H]\{\beta\} - \lfloor\beta\rfloor [T]\{q\} \tag{11}$$

where
$$[T] = \int_{A_2} [R^T] [L] dA \tag{12}$$

Use of the principle of minimum complementary energy (i.e., $\frac{\partial \pi_c}{\partial \beta_i} = 0,\ i = 1, \ldots\ldots m$) yields:

$$[H] \{\beta\} = [T] \{q\} \tag{13}$$

or
$$\{\beta\} = [H^{-1}] [T] \{q\} \tag{14}$$

Substituting $\{\beta\}$ into eq.(7) one obtains:

$$U = \frac{1}{2} \lfloor q\rfloor [T^T] [H^{-1}] [T] \{q\} \tag{15}$$

Comparing eqs. (1) and (15), one can obtain the element stiffness matrix as:

$$[k] = [T^T] [H^{-1}] [T] \tag{16}$$

It is seen that the generalized forces $\{Q\}$ are given by:

$$\{Q\} = [k]\{q\} \tag{17}$$

Substituting $[k]$ from eq.(16) and then using eq.(14), one finds:

$$\{Q\} = [T^T]\{\beta\} \tag{18}$$

The matrix $[T^T]$ thus relates the equivalent generalized forces $\{Q\}$ and the assumed stress coefficients $\{\beta\}$.

It is seen from eq.(5) that it is possible to incorporate the prescribed stresses on the boundary of an element by suitably adjusting the number of unknown stress coefficients $\{\beta\}$ for the element.

Actual assumption of the stress pattern used in this report to formulate the element stiffness matrices for triangular and quadrilateral elements is given by:

$$\begin{aligned}
\sigma_z &= \beta_1 - \beta_4 \frac{z}{r} + \frac{1}{6}\beta_8 \frac{z^3}{r^3} \\
\sigma_r &= \beta_2 + \frac{\beta_5}{r^2} + \frac{\beta_6}{r^3} + \beta_7 \frac{z}{r} \\
\sigma_\theta &= \beta_3 - \frac{\beta_5}{r^2} - 2\frac{\beta_6}{r^3} + \beta_8 \frac{z}{r} \\
\tau_{rz} &= \beta_4 + (\beta_3 - \beta_2)\frac{z}{r} + \frac{\beta_8}{2}\frac{z^2}{r^2}
\end{aligned} \tag{19}$$

It can be easily verified that the stresses assumed above satisfy the equations of equilibrium [11] derived for an axisymmetric body subjected to axisymmetric loading, i.e., they satisfy

$$\begin{aligned}
\frac{\partial \sigma_r}{\partial r} + \frac{\partial \tau_{rz}}{\partial z} + \frac{\sigma_r - \sigma_\theta}{r} &= 0 \\
\frac{\partial \sigma_z}{\partial z} + \frac{\partial \tau_{rz}}{\partial r} + \frac{\tau_{rz}}{r} &= 0
\end{aligned} \tag{20}$$

Moreover, it is seen from eq.(19) that the functions $\frac{1}{r^2}$ and $\frac{1}{r^3}$ which appear in the classical solution for thick cylinders and thick spheres respectively are used in the assumption for stresses. It is to be noted here that the coordinate system adopted in the finite element analysis of arbitrary shaped axisymmetric bodies (r, z, θ) is not the same as that used in the solution for the thick sphere (r, θ). From eq.(19), the matrix $[P]$ is given by:

$$[P] = \begin{bmatrix} 1 & 0 & 0 & -\frac{z}{r} & 0 & 0 & 0 & \frac{z^3}{6r^3} \\ 0 & 1 & 0 & 0 & \frac{1}{r^2} & \frac{1}{r^3} & \frac{z}{r} & 0 \\ 0 & 0 & 1 & 0 & -\frac{1}{r^2} & -\frac{2}{r^3} & 0 & \frac{z}{r} \\ 0 & -\frac{z}{r} & \frac{z}{r} & 1 & 0 & 0 & 0 & \frac{z^2}{2r^2} \end{bmatrix} \quad (21)$$

for

$$\{\sigma\} = \begin{Bmatrix} \sigma_z \\ \sigma_r \\ \sigma_\theta \\ \tau_{rz} \end{Bmatrix} \quad \text{and} \quad \{\beta\} = \begin{Bmatrix} \beta_1 \\ \beta_2 \\ \vdots \\ \beta_8 \end{Bmatrix} \quad (22)$$

Assuming an isotropic material the matrix $[N]$ is given by:

$$[N] = \frac{1}{E} \begin{bmatrix} 1 & -\nu & -\nu & 0 \\ -\nu & 1 & -\nu & 0 \\ -\nu & -\nu & 1 & 0 \\ 0 & 0 & 0 & 2(1+\nu) \end{bmatrix} \quad (23)$$

where E is the Young's Modulus and ν is the Poisson's ratio.

The surface force matrix $\{S\}$ is given by (Fig.3):

For a triangle: $$\{S\} = \begin{Bmatrix} \bar{R}_{12} \\ \bar{Z}_{12} \\ \bar{R}_{23} \\ \bar{Z}_{23} \\ \bar{R}_{31} \\ \bar{Z}_{31} \end{Bmatrix} = \begin{Bmatrix} \sigma_r s_1 - \tau_{rz} c_1 \\ -\sigma_z c_1 + \tau_{rz} s_1 \\ \sigma_r s_2 - \tau_{rz} c_2 \\ -\sigma_z c_2 + \tau_{rz} s_2 \\ \sigma_r s_3 - \tau_{rz} c_3 \\ -\sigma_z c_3 + \tau_{rz} s_3 \end{Bmatrix} \quad (24)$$

for a quadrilateral: $\{S\} = \begin{Bmatrix} \bar{R}_{12} \\ \bar{Z}_{12} \\ \bar{R}_{23} \\ \bar{Z}_{23} \\ \bar{R}_{34} \\ \bar{Z}_{34} \\ \bar{R}_{41} \\ \bar{Z}_{41} \end{Bmatrix} = \begin{Bmatrix} \sigma_r s_1 - \tau_{rz} c_1 \\ -\sigma_z c_1 + \tau_{rz} s_1 \\ \sigma_r s_2 - \tau_{rz} c_2 \\ -\sigma_z c_2 + \tau_{rz} s_2 \\ \sigma_r s_3 - \tau_{rz} c_3 \\ -\sigma_z c_3 + \tau_{rz} s_3 \\ \sigma_r s_4 - \tau_{rz} c_4 \\ -\sigma_z c_4 + \tau_{rz} s_4 \end{Bmatrix}$ (25)

where $s_i = \sin\theta_i$ and $c_i = \cos\theta_i$

Linear variation of $\{u\}$ displacements is prescribed on the surface of the elements so that the inter-element compatibility is achieved. Displacement matrix $\{u\}$ is given by (Fig.4):

for a triangle: $\{u\} = \begin{Bmatrix} u_r^{12} \\ u_z^{12} \\ u_r^{23} \\ u_z^{23} \\ u_r^{31} \\ u_z^{31} \end{Bmatrix} = \begin{Bmatrix} q_1 + (q_3 - q_1)\, x_1 \\ q_2 + (q_4 - q_2)\, x_1 \\ q_3 + (q_5 - q_3)\, x_2 \\ q_4 + (q_6 - q_4)\, x_2 \\ q_5 + (q_1 - q_5)\, x_3 \\ q_6 + (q_2 - q_6)\, x_3 \end{Bmatrix}$ (26)

for a quadrilateral: $\{u\} = \begin{Bmatrix} u_r^{12} \\ u_z^{12} \\ u_r^{23} \\ u_z^{23} \\ u_r^{34} \\ u_z^{34} \\ u_r^{41} \\ u_z^{41} \end{Bmatrix} = \begin{Bmatrix} q_1 + (q_3 - q_1)\, x_1 \\ q_2 + (q_4 - q_2)\, x_1 \\ q_3 + (q_5 - q_3)\, x_2 \\ q_4 + (q_6 - q_4)\, x_2 \\ q_5 + (q_7 - q_5)\, x_3 \\ q_6 + (q_8 - q_6)\, x_3 \\ q_7 + (q_1 - q_7)\, x_4 \\ q_8 + (q_2 - q_8)\, x_4 \end{Bmatrix}$ (27)

where $x_1 = \frac{l_{rz1}}{l_{12}}$, $x_2 = \frac{l_{rz2}}{l_{23}}$, $x_3 = \frac{l_{rz3}}{l_{31}}$, $x_3' = \frac{l_{rz3}}{l_{34}}$, and $x_4 = \frac{l_{rz4}}{l_{41}}$

and in which $l_{rzi} = \sqrt{(r-r_i)^2 + (z-z_i)^2}$

and $l_{jk} = \sqrt{(r_k-r_j)^2 + (z_k-z_j)^2}$

The matrix $[H]$ and the matrices $[T]$ for the triangle and quadrilateral elements are worked out for the stress assumption given above and are given in Figs.5 through 7 respectively. It can be seen from the matrices $[T]$ that columns 3 through 8 can be written from the terms of columns 1 and 2 by changing the subscripts suitably.

4. EXAMPLE PROBLEMS AND RESULTS OF ANALYSIS

Two example problems were analyzed using the assumed stress hybrid model - (i) a thick sphere subjected to internal pressure (Fig.8) by using triangular elements, and (ii) an infinitely long thick cylinder subjected to internal pressure (Fig.9) by using triangular and quadrilateral elements. Gaussian quadrature method of numerical integration was used to evaluate the matrices $[H]$ and $[T]$.

Figs.10 and 11 show the σ_r and σ_θ stresses across the wall of the thick sphere obtained by using the assumed stress hybrid model and the assumed displacement model. The exact solution for the stresses is also shown in the same figures. Deflections of the inner and outer faces of the sphere obtained by using the assumed stress hybrid model are shown in Fig.12 along with the exact solution.

Similarly, stresses across the wall of the thick cylinder are shown in Figs.13 and 14; and deflection of the points A and B (Fig.9) are shown in Table I.

It is to be noted that all the stresses shown in Figs.10,11,13, and 14 are either nodal average stresses or centroidal stresses.

5. DISCUSSION AND REMARKS

It is seen from Figs.10,11,13, and 14 that σ_r stresses at the inner faces of the thick sphere and the thick cylinder obtained by using the assumed stress hybrid model are closer to the exact values than the stresses obtained by the assumed displacement model. Moreover, for the assumed stress hybrid model, the σ_r stress at the inner face of the cylinder obtained by using five quadrilateral elements is better than the stress obtained by using twenty nine triangular elements. As already mentioned in section 3, it is also possible to exactly satisfy the boundary stress condition for an assumed stress hybrid model by suitably adjusting the number of stress coefficients $\{\beta\}$ for the elements on the boundary. Deflections and σ_θ stresses obtained by the assumed stress model are nearly the same as those obtained by using the assumed displacement model. However, it is to be noted that the number of calculations required to compute an element stiffness matrix in the case of the assumed stress model are more than in the case of the assumed displacement model. On the other hand, it is quite straight forward to formulate an element stiffness matrix with boundary compatibility for any assumed stress pattern which satisfies the equilibrium.

From the above discussion it can be stated that the assumed stress model presented in this report confirms the conclusion drawn by Pian that the finite element method based on the assumed stress method can provide more accurate stress estimation than the assumed displacement schemes.

ACKNOWLEDGMENTS

The author wishes to express his gratitude to Prof.G.S. Ramaswamy, Director, Structural Engineering Research Centre, Roorkee (India), and to Mr.M. Ramaiah, Scientist-in-charge, Structural Engineering Research (Regional) Centre, Madras (India), for the encouragement and help given by them during the period of work to produce this report and for permitting this report to be published.

REFERENCES

[1] CLOUGH, R.W., RASHID, Y.R., "Finite Element Analysis of Axi-Symmetric Solids", ASCE, Engg. Mech. Div. Journal, Vol.91, No.EM 1, pp 71-85, Feb.'65.

[2] WILSON, E.L., "Structural Analysis of Axisymmetric Solids", AIAA Journal, pp 2269-74, Jan. 1965.

[3] CLOUGH, R.W., "The Finite Element Method in Structural Mechanics", Ch.7. Stress Analysis, edited by O.C.Zienkiewicz and G.S. Hollister, Wiley, New York 1965.

[4] ZIENKIEWICZ, O.C., CHEUNG, Y.K., The Finite Element Method in Structural and Continuum Mechanics, McGraw-Hill, 1967.

[5] ZIENKIEWICZ, O.C., WATSON, M., CHEUNG, Y.K., "Stress Analysis by the Finite Element Method - Thermal effects", paper No.35, Proceedings of the Conference on Prestressed Concrete Pressure Vessels, March '67, London.

[6] PIAN, T.H.H., "Derivation of Element Stiffness Matrices by Assumed Stress Distributions", AIAA Journal, Vol.2, pp 1333-1336 (1964).

[7] COOK, R.D., AL-ABDULLA, J.K., "Some Plane Quadrilateral Hybrid Finite Elements", Tech. Note, AIAA Journal, pp 2184-2185, Nov. '69.

[8] PIAN, T.H.H., "Element Stiffness Matrices for Boundary Compatibility and Prescribed Boundary Stresses", in session 3, Proceedings of the Conference on Matrix Methods in Structural Mechanics, Wright-Patterson Air Force Base, Ohio, Oct. '65.

[9] PIAN, T.H.H., TONG, P., "Basis of Finite Element Methods for Solid Continua", International Journal for Numerical Methods in Engineering, Vol.I, pp 3-28 (1969).

[10] SOKOLNIKOFF, I.S., Mathematical Theory of Elasticity, 2nd ed., ch.7, p 387, New York, 1956.

[11] TIMOSHENKO, S.P., GOODIER, J.H., Theory of Elasticity, McGraw Hill.

Table I Deflections of the thick cylinder

Location	Displ. Approx. (Fig.9b)	Stress Approx. (Fig.9b)	Displ. Approx. (Fig.9c)	Stress Approx. (Fig.9c)	Stress Approx. (Fig.9a)	Exact Sol.
A	0.0177	0.0178	0.0177	0.0177	0.0178	0.0180
B	0.0080	0.0080	0.0080	0.0080	0.0080	0.0083

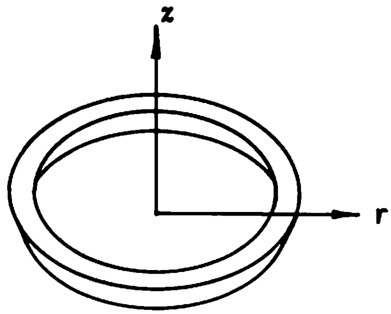

(a) A TRIANGULAR RING ELEMENT

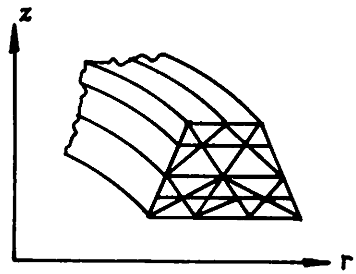

(b) IDEALIZATION OF AN AXISYMMETRIC SOLID INTO TRIANGULAR RING ELEMENTS

Fig.1 Idealization into triangular ring elements

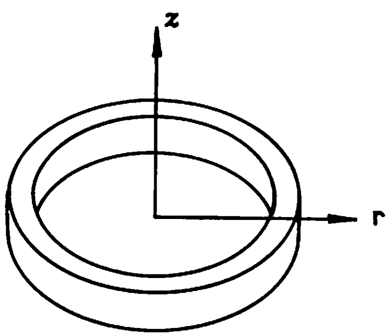

(a) A QUADRILATERAL RING ELEMENT

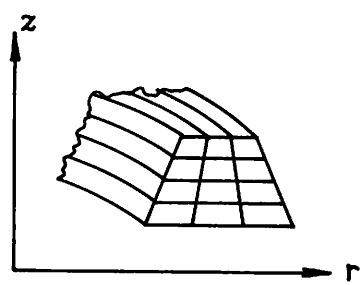

(b) IDEALIZATION OF AN AXISYMMETRIC SOLID INTO QUADRILATERAL RING ELEMENTS

Fig.2 Idealization into quadrilateral ring elements

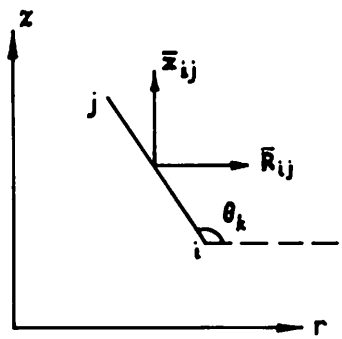

Fig.3 Surface forces on the side ij

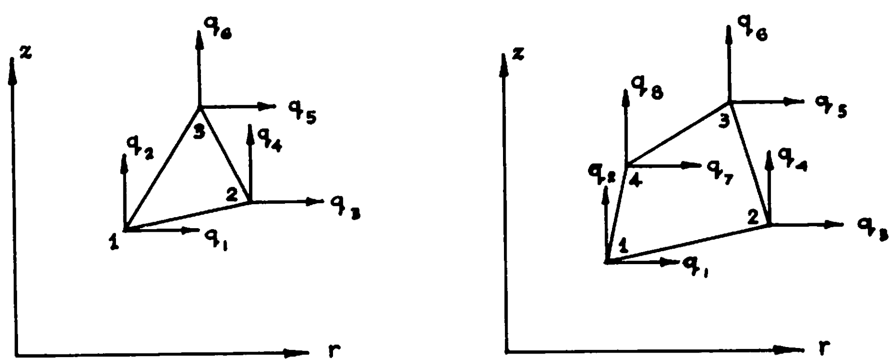

Fig.4 Nodal displacements

$$[H] = \int_V \frac{1}{E} \begin{bmatrix} 1 & -\nu & -\nu & -\frac{z}{r} & 0 & \frac{\nu}{r^3} & -\frac{\nu z}{r} & \frac{z^3}{6r^3} - \frac{\nu z}{r} \\ & 1+2(1+\nu)\frac{z^2}{r^2} & -\nu - 2(1+\nu)\frac{z^2}{r^2} & -\frac{z}{r}(2+\nu) & \frac{(1+\nu)}{r^2} & \frac{(1+2\nu)}{r^3} & \frac{z}{r} & -\frac{\nu z}{r} - \frac{z^3}{r^3}\left(1+\frac{7}{6}\nu\right) \\ & & 1+2(1+\nu)\frac{z^2}{r^2} & \frac{z}{r}(2+3\nu) & -\frac{1}{r^2}(1+\nu) & -\frac{1}{r^3}(2+\nu) & -\frac{\nu z}{r} & \frac{z}{r} + \frac{z^3}{r^3}\left(1+\frac{5}{6}\nu\right) \\ & & & \frac{z^2}{r^2} + 2(1+\nu) & 0 & -\frac{\nu z}{r^4} & \nu\frac{z^2}{r^2} & (1+2\nu)\frac{z^2}{r^2} - \frac{z^4}{6r^4} \\ & \text{symmetric} & & & \frac{2(1+\nu)}{r^4} & \frac{3(1+\nu)}{r^6} & \frac{z(1+\nu)}{r^3} & \frac{-z(1+\nu)}{r^3} \\ & & & & & \frac{(5+4\nu)}{r^6} & \frac{z(1+2\nu)}{r^4} & \frac{\nu z^3}{6r^6} - (\nu+2)\frac{z}{r^4} \\ & & & & & & \frac{z^2}{r^2} & \frac{-\nu z^4}{6r^4} - \frac{\nu z^2}{r^2} \\ & & & & & & & \frac{z^6}{36r^6} + \frac{z^4(3+\nu)}{6r^4} + \frac{z^2}{r^2} \end{bmatrix} dv$$

Fig.5 Matrix [H]

$$
[T] = \int_{A_2} \begin{pmatrix}
0 & r(c_1x_1-c_1-c_3x_3) & 0 & r(c_2x_2-c_2-c_1x_1) & 0 & r(c_3x_3-c_3-c_2x_2) \\
\begin{matrix} r(b_1-b_1x_1+b_3x_3) \\ +z(c_1-c_1x_1+c_3x_3) \end{matrix} & z(b_1x_1-b_1-b_3x_3) & \begin{matrix} r(b_2-b_2x_2+b_1x_1) \\ +z(c_2-c_2x_2+c_1x_1) \end{matrix} & z(b_2x_2-b_2-b_1x_1) & \begin{matrix} r(b_3-b_3x_3+b_2x_2) \\ +z(c_3-c_3x_3+c_2x_2) \end{matrix} & z(b_3x_3-b_3-b_2x_2) \\
z(c_1x_1-c_1-c_3x_3) & z(b_1-b_1x_1+b_3x_3) & z(c_2x_2-c_2-c_1x_1) & z(b_2-b_2x_2+b_1x_1) & z(c_3x_3-c_3-c_2x_2) & z(b_3-b_3x_3+b_2x_2) \\
r(c_1x_1-c_1-c_3x_3) & \begin{matrix} r(b_1-b_1x_1+b_3x_3) \\ +z(c_1-c_1x_1+c_3x_3) \end{matrix} & r(c_2x_2-c_2-c_1x_1) & \begin{matrix} r(b_2-b_2x_2+b_1x_1) \\ +z(c_2-c_2x_2+c_1x_1) \end{matrix} & r(c_3x_3-c_3-c_2x_2) & \begin{matrix} r(b_3-b_3x_3+b_2x_2) \\ +z(c_3-c_3x_3+c_2x_2) \end{matrix} \\
\frac{1}{r}(b_1-b_1x_1+b_3x_3) & 0 & \frac{1}{r}(b_2-b_2x_2+b_1x_1) & 0 & \frac{1}{r}(b_3-b_3x_3+b_2x_2) & 0 \\
\frac{1}{r^2}(b_1-b_1x_1+b_3x_3) & 0 & \frac{1}{r^2}(b_2-b_2x_2+b_1x_1) & 0 & \frac{1}{r^2}(b_3-b_3x_3+b_2x_2) & 0 \\
z(b_1-b_1x_1+b_3x_3) & 0 & z(b_2-b_2x_2+b_1x_1) & 0 & z(b_3-b_3x_3+b_2x_2) & 0 \\
\frac{z^2}{2r}(c_1x_1-c_1-c_3x_3) & \begin{matrix} \frac{z^3}{6r^2}(c_1x_1-c_1-c_3x_3) \\ +\frac{z^2}{2r}(b_1-b_1x_1+b_3x_3) \end{matrix} & \frac{z^2}{2r}(c_2x_2-c_2-c_1x_1) & \begin{matrix} \frac{z^3}{6r^2}(c_2x_2-c_2-c_1x_1) \\ +\frac{z^2}{2r}(b_2-b_2x_2+b_1x_1) \end{matrix} & \frac{z^2}{2r}(c_3x_3-c_3-c_2x_2) & \begin{matrix} \frac{z^3}{6r^2}(c_3x_3-c_3-c_2x_2) \\ +\frac{z^2}{2r}(b_3-b_3x_3+b_2x_2) \end{matrix}
\end{pmatrix} dA
$$

Fig.6 Matrix $[T]$ for the triangular element

$$
[T] = \int_{A_2} \begin{bmatrix}
0 & r(c_1X_1-c_1-c_4X_4) & 0 & r(c_2X_2-c_2-c_1X_1) & 0 & r(c_3X_3'-c_3-c_2X_2) & 0 & r(c_4X_4-c_4-c_3X_3') \\
\begin{matrix} r(s_1-s_1X_1+s_4X_4) \\ +z(c_1-c_1X_1+c_4X_4) \end{matrix} & z(s_1X_1-s_1-s_4X_4) & \begin{matrix} r(s_2-s_2X_2+s_1X_1) \\ +z(c_2-c_2X_2+c_1X_1) \end{matrix} & z(s_2X_2-s_2-s_1X_1) & \begin{matrix} r(s_3-s_3X_3'+s_2X_2) \\ +z(c_3-c_3X_3'+c_2X_2) \end{matrix} & z(s_3X_3'-s_3-s_2X_2) & \begin{matrix} r(s_4-s_4X_4+s_3X_3') \\ +z(c_4-c_4X_4+c_3X_3') \end{matrix} & z(s_4X_4-s_4-s_3X_3') \\
z(c_1X_1-c_1-c_4X_4) & z(s_1-s_1X_1+s_4X_4) & z(c_2X_2-c_2-c_1X_1) & z(s_2-s_2X_2+s_1X_1) & z(c_3X_3'-c_3-c_2X_2) & z(s_3-s_3X_3'+s_2X_2) & z(c_4X_4-c_4-c_3X_3') & z(s_4-s_4X_4+s_3X_3') \\
r(c_1X_1-c_1-c_4X_4) & \begin{matrix} z(c_1-c_1X_1+c_4X_4) \\ +r(s_1-s_1X_1+s_4X_4) \end{matrix} & r(c_2X_2-c_2-c_1X_1) & \begin{matrix} z(c_2-c_2X_2+c_1X_1) \\ +r(s_2-s_2X_2+s_1X_1) \end{matrix} & r(c_3X_3'-c_3-c_2X_2) & \begin{matrix} z(c_3-c_3X_3'+c_2X_2) \\ +r(s_3-s_3X_3'+s_2X_2) \end{matrix} & r(c_4X_4-c_4-c_3X_3') & \begin{matrix} z(c_4-c_4X_4+c_3X_3') \\ +r(s_4-s_4X_4+s_3X_3') \end{matrix} \\
\frac{1}{r}(s_1-s_1X_1+s_4X_4) & 0 & \frac{1}{r}(s_2-s_2X_2+s_1X_1) & 0 & \frac{1}{r}(s_3-s_3X_3'+s_2X_2) & 0 & \frac{1}{r}(s_4-s_4X_4+s_3X_3') & 0 \\
\frac{1}{r^2}(s_1-s_1X_1+s_4X_4) & 0 & \frac{1}{r^2}(s_2-s_2X_2+s_1X_1) & 0 & \frac{1}{r^2}(s_3-s_3X_3'+s_2X_2) & 0 & \frac{1}{r^2}(s_4-s_4X_4+s_3X_3') & 0 \\
z(s_1-s_1X_1+s_4X_4) & 0 & z(s_2-s_2X_2+s_1X_1) & 0 & z(s_3-s_3X_3'+s_2X_2) & 0 & z(s_4-s_4X_4+s_3X_3') & 0 \\
\frac{z^2}{2r}(c_1X_1-c_1-c_4X_4) & \begin{matrix} \frac{z^3}{6r^2}(c_1X_1-c_1-c_4X_4) \\ +\frac{z^2}{2r}(s_1-s_1X_1+s_4X_4) \end{matrix} & \frac{z^2}{2r}(c_2X_2-c_2-c_1X_1) & \begin{matrix} \frac{z^3}{6r^2}(c_2X_2-c_2-c_1X_1) \\ +\frac{z^2}{2r}(s_2-s_2X_2+s_1X_1) \end{matrix} & \frac{z^2}{2r}(c_3X_3'-c_3-c_2X_2) & \begin{matrix} \frac{z^3}{6r^2}(c_3X_3'-c_3-c_2X_2) \\ +\frac{z^2}{2r}(s_3-s_3X_3'+s_2X_2) \end{matrix} & \frac{z^2}{2r}(c_4X_4-c_4-c_3X_3') & \begin{matrix} \frac{z^3}{6r^2}(c_4X_4-c_4-c_3X_3') \\ +\frac{z^2}{2r}(s_4-s_4X_4+s_3X_3') \end{matrix}
\end{bmatrix} dA
$$

Fig.7 Matrix $[T]$ for the quadrilateral element

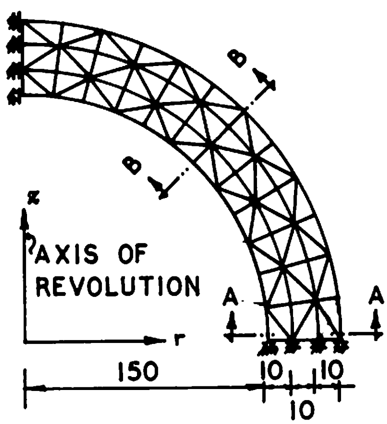

UNIT INTERNAL PRESSURE

POISSON'S RATIO $\nu = 0.17$

Fig.8 Idealization for the thick sphere problem

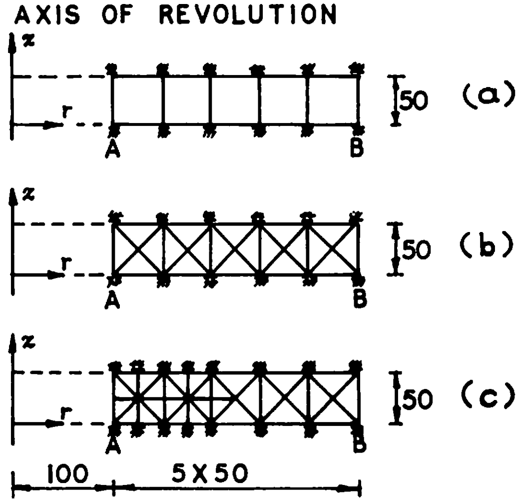

INTERNAL PRESSURE 60 UNITS

POISSION'S RATIO $\nu = 0.17$

Fig.9 Idealizations for the thick cylinder problem

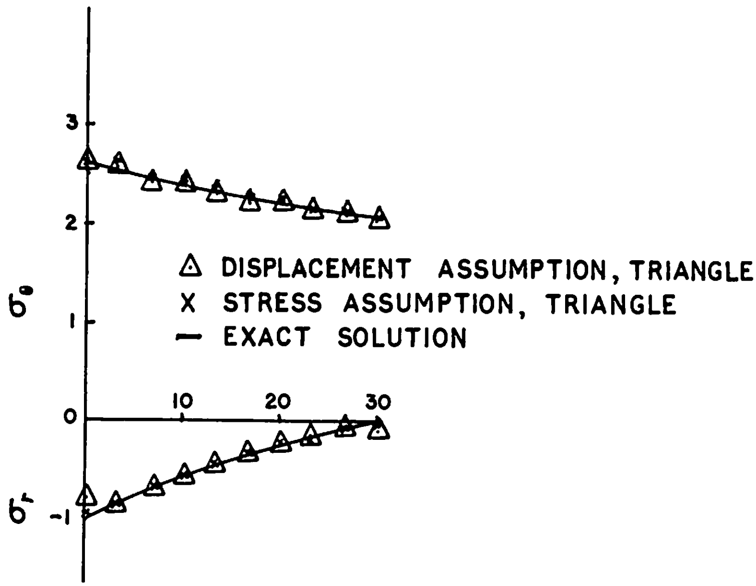

Fig.10 Stresses in the thick sphere across the section AA

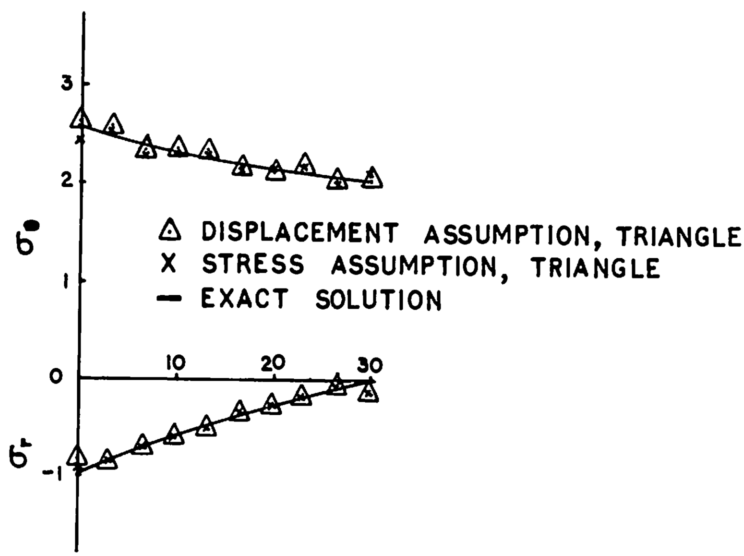

Fig.11 Stresses in the thick sphere across the section BB

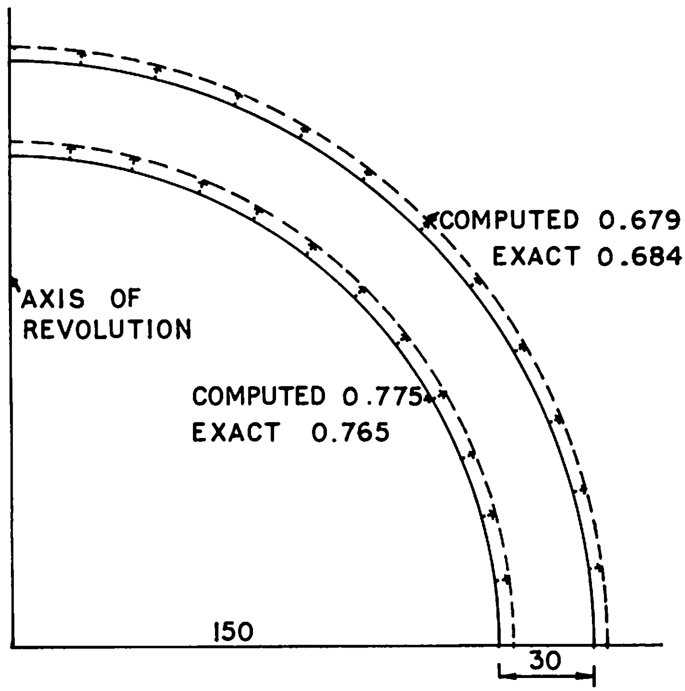

Fig. 12 Deflections of the inner and outer faces of the thick sphere

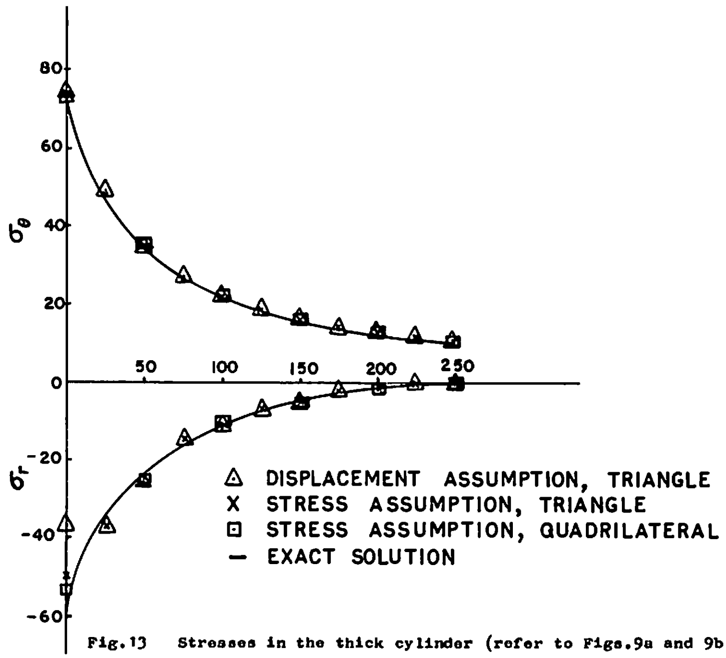

Fig. 13 Stresses in the thick cylinder (refer to Figs. 9a and 9b)

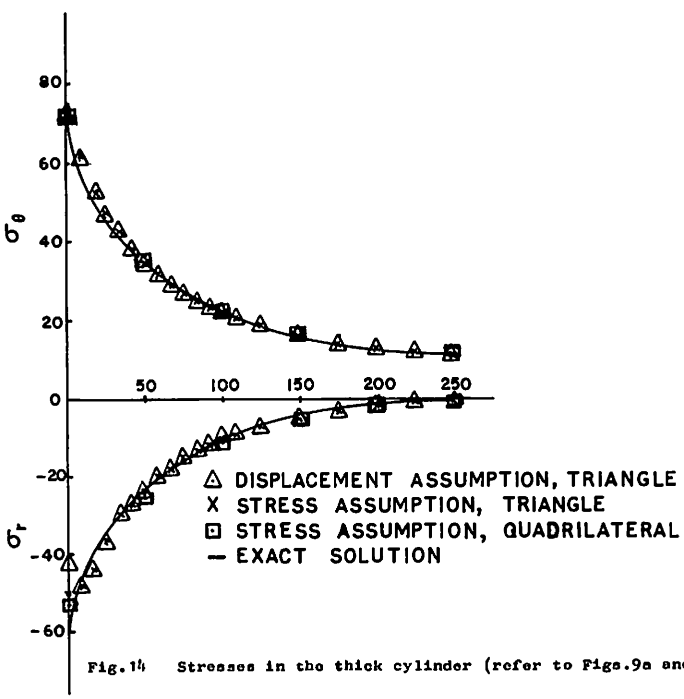

Fig. 14 Stresses in the thick cylinder (refer to Figs. 9a and 9c)

DISCUSSION

Q J. A. SWANSON, U. S. A.

The major difference between the stress and displacement models is in the stress at the surface. Agreement internally is good. It appears a better surface stress calculation is needed.

A technique used in the ANSYS program is the calculation of the surface stress conditions directly from the surface displacements. The technique is as follows:

Known: u_r, u_z at two surface nodal points I, J

$$\left.\begin{array}{l}\sigma_n = \text{applied pressure} \\ \tau_{nt} = 0.0\end{array}\right\} \text{surface properties}$$

$$\varepsilon_\theta = \frac{u_I + u_j}{r_I + r_J} \qquad \varepsilon_t = \frac{u_{tJ} - u_{tI}}{\sqrt{(r_I - r_J)^2 + (z_I - z_J)^2}}$$

$$\left.\begin{array}{l}\tau_{t\theta} = 0.0 \\ \tau_{n\theta} = 0.0\end{array}\right\} \text{for axisymmetric bodies}$$

n = normal direction r = radial direction

t = tangential direction z = axial direction.

From these six conditions the complete stress distribution at the surface can be obtained, without extrapolation.

A similar technique is used in ANSYS for three dimensional solids.

A T. V. S. R. APPA RAO, India

I agree with your comment that the difference between stress and displacement models is in the stress at the surface. I am happy to note the method of calculating the surface stress condition from the surface displacements. It seems to avoid the extrapolation otherwise necessary.

C J. T. ODEN, U. S. A.

I would like to comment that the use of the concept of consistent or conjugate stress approximations in displacement finite element models overcomes many of the traditional criticisms of stresses computed from approximate displacement fields. Indeed, for a conforming displacement approximation, the method leads to a continuous description of stress which can be shown to be the better, in a mean square sense, than averaged stresses written as linear combinations of the displacement weight functions. Details can be found in a recent issue of the International Journal of Numerical Methods in Engineering.